Nuclear Physics **A359** (1981) 331–348
© North-Holland Publishing Company

PHENOMENOLOGICAL TWO-NUCLEON INTERACTION OPERATOR*

I.E. LAGARIS and V.R. PANDHARIPANDE

Department of Physics, University of Illinois at Urbana-Champaign, Urbana, IL 61801, USA

Received 27 August 1980

Abstract: We report a phenomenological two-nucleon interaction operator obtained by fitting the nucleon–nucleon phase shifts up to 425 MeV in S, P, D and F waves, and the deuteron properties. The operator has the standard eight potentials associated with the two-body operators 1, $\sigma_1 \cdot \sigma_2$, $\tau_1 \cdot \tau_2$, $\sigma_1 \cdot \sigma_2 \tau_1 \cdot \tau_2$, S_{12}, $S_{12}\tau_1 \cdot \tau_2$, $\boldsymbol{L} \cdot \boldsymbol{S}$ and $\boldsymbol{L} \cdot \boldsymbol{S}\tau_1 \cdot \tau_2$; and six phenomenological potentials associated with operators L^2, $L^2\sigma_1 \cdot \sigma_2$, $L^2\tau_1 \cdot \tau_2$, $L^2\sigma_1 \cdot \sigma_2\tau_1 \cdot \tau_2$, $(\boldsymbol{L} \cdot \boldsymbol{S})^2$ and $(\boldsymbol{L} \cdot \boldsymbol{S})^2\tau_1 \cdot \tau_2$. The six "quadratic L" terms are relatively weak, and are chosen in order to make many-body calculations with this operator simpler.

1. Introduction

In many-body calculations of nuclei and nuclear matter it is convenient to represent the two-nucleon interaction as an operator:

$$v_{ij} = \sum_p v^p(r_{ij}) O_{ij}^p, \tag{1.1}$$

where $v^p(r_{ij})$ are functions of the interparticle distance r_{ij}, and O_{ij}^p are conveniently chosen operators. The nucleon–nucleon (NN) scattering data uniquely indicate the occurrence of terms belonging to the eight operators:

$$O_{ij}^{p=1,8} = 1, \sigma_i \cdot \sigma_j, \tau_i \cdot \tau_j, (\sigma_i \cdot \sigma_j)(\tau_i \cdot \tau_j), S_{ij}, S_{ij}(\tau_i \cdot \tau_j), (\boldsymbol{L} \cdot \boldsymbol{S})_{ij}, (\boldsymbol{L} \cdot \boldsymbol{S})_{ij}(\tau_i \cdot \tau_j) \tag{1.2}$$

in the v_{ij}. Here S_{ij} is the tensor operator, $\boldsymbol{L}$ the relative angular momentum, and $\boldsymbol{S}$ the total spin of the pair.

Many nuclear matter calculations have been done with "Bethe's v_8 homework" models obtained by assuming that the interaction in all pair isospin-spin $T, S = 1, 0$; 0, 0; 0, 1 and 1, 1 states is given respectively by that in the $^1S_0$, $^1P_1$, ($^3S_1$-$^3D_1$) and ($^3P_2$-$^3F_2$) channels. These models have only the above eight terms in their interaction operators. Unfortunately the v_8 models, based on potentials such as those of Reid [1]) and Bethe-Johnson [2]) etc., do not generally give good phase shifts in the $^3P_0$, $^3P_1$, $^1D_2$, $^3D_2$ and $^3D_3$ states.

The Paris group [3]) has attempted to cast its model of NN interaction in the form (1.1). In addition to the terms belonging to the eight operators (1.2) they have taken

* Supported by NSF PHY 78-26582.

four momentum-dependent terms:

$$\sum_{T=0,1;S=0,1} (\nabla^2 v^k_{T,S}(r_{ij}) + v^k_{T,S}(r_{ij})\nabla^2) P^{T,S}, \tag{1.3}$$

where $P^{T,S}$ is a projection operator; and two terms quadratic in $\boldsymbol{L}$:

$$\sum_{T=0,1} v_T^{S02}(r_{ij})(\sigma_i \cdot \boldsymbol{L}\sigma_j \cdot \boldsymbol{L} + \sigma_j \cdot \boldsymbol{L}\sigma_i \cdot \boldsymbol{L}) P^T. \tag{1.4}$$

The Paris potential gives a satisfactory fit to the scattering data. However, the momentum-dependent terms in the Paris potential are very strong. As a matter of fact they give the dominant contribution to the energy of nuclear matter. At Fermi momenta $k_F = 1.6\ \text{fm}^{-1}$ the four momentum-dependent terms give ≈ -40 MeV per nucleon to make the matter bound with a binding energy of ~ -20 MeV per nucleon. If we let the interaction (1.3) operate on the right hand ψ we get three terms which respectively contain $(\nabla^2 v^k)\psi$, $2\nabla v^k \cdot \nabla\psi$ and $2v^k\nabla^2\psi$. The first term gives a contribution of ~ -80 MeV that can be accurately calculated. The latter two terms give $\sim +40$ MeV per nucleon at $k_F = 1.6\ \text{fm}^{-1}$. It is difficult to calculate their contribution [4]) and it is risky to use approximations when it is so large.

There are no compelling reasons to believe that the NN interaction has indeed such a large momentum dependence. Hence it is worthwhile to explore other parameterizations of the NN interaction operator, which explain the two-body data and whose dominant contributions are associated with the eight operators (1.2). In the present work we report a v_{14} model of NN interaction that satisfies these requirements. Nuclear matter calculations with this model will be reported elsewhere [5]).

The six additional terms in our model are associated with the operators:

$$O_{ij}^{p=9,14} = L^2, L^2(\sigma_1 \cdot \sigma_2), L^2(\tau_1 \cdot \tau_2), L^2(\sigma_1 \cdot \sigma_2)(\tau_1 \cdot \tau_2), (\boldsymbol{L} \cdot \boldsymbol{S})^2, (\boldsymbol{L} \cdot \boldsymbol{S})^2(\tau_1 \cdot \tau_2). \tag{1.5}$$

Instead of the numbers 1–14 we often use letters, c, σ, τ, $\sigma\tau$, t, tτ, b, bτ, q, qσ, qτ, q$\sigma\tau$, bb and bbτ as subscripts/superscripts to denote functions associated with these operators. In this notation, σ, τ, t, b and q, respectively, stand for $\sigma_i \cdot \sigma_j$, $\tau_i \cdot \tau_j$, S_{ij}, $(\boldsymbol{L} \cdot \boldsymbol{S})_{ij}$ and L^2. The operators (1.5) were chosen to simplify the many-body calculations.

Our potentials contain the well-known one-pion-exchange interaction; and an intermediate range attraction that is modeled to give the second-order contributions of one-pion-exchange transition potentials that excite nucleons to isobar states [6,7]). The short-range interaction is purely phenomenological. The terms containing L^2 and $(\boldsymbol{L} \cdot \boldsymbol{S})^2$ operators are relatively weak. They give +6.4 MeV contribution to the energy of nuclear matter at $k_F = 1.6\ \text{fm}^{-1}$, and it is only +2.4 MeV at the equilibrium $k_F = 1.33\ \text{fm}^{-1}$.

The parametrization of the potential and the phase shift fits are reported in sect. 2, while the deuteron properties are reported in sect. 3.

2. The v_{14} interaction model

The two-nucleon interaction is written as:

$$v_{ij} = \sum_{p=1,14} (v_\pi^p(r_{ij}) + v_I^p(r_{ij}) + v_S^p(r_{ij}))O_{ij}^p . \tag{2.1}$$

The one-pion-exchange $v_\pi^p(r_{ij})$ is non-zero only for $p = \sigma\tau$ and $t\tau$:

$$v_\pi^{\sigma\tau}(r) = 3.488 \frac{e^{-0.7r}}{0.7r}(1 - e^{-cr^2}) , \tag{2.2}$$

$$v_\pi^{t\tau}(r) = 3.488\left(1 + \frac{3}{0.7r} + \frac{3}{(0.7r)^2}\right)\frac{e^{-0.7r}}{0.7r}(1 - e^{-cr^2})^2 , \tag{2.3}$$

$$\equiv 3.448 T_\pi(r) . \tag{2.4}$$

The $1/r$ and $1/r^3$ singularities of the one-pion-exchange potential are removed, and the cut-off parameter c is determined by fitting the phase shifts. Green and Haapakoski [8]) have recommended the $(1 - e^{-cr^2})^2$ cut off arguing that it simulates the effect of ρ-exchange interaction. We have cut off the Yukawa shaped $v_\pi^{\sigma\tau}(r)$ purely because the quark models suggest that the nucleon is not a point source, and so the two-nucleon interaction should not have a $1/r$ behavior at small r.

The $v_I^p(r_{ij})$ is attributed to second-order, one-pion-exchange transition potentials. So its radial dependence should approximately be given by $T_\pi^2(r)$, and we take:

$$v_I^p(r_{ij}) = I^p T_\pi^2(r) . \tag{2.5}$$

This choice of v_I also makes it simpler to introduce effects of three-nucleon interactions [5]). The strengths I^p are determined by fitting the phase shifts.

Traditionally the short-range interaction $v_S^p(r_{ij})$ is attributed to ω, ρ exchange, and taken to have a Yukawa shape. However, since the believed size of nucleon is at least of the order of the Compton wave length of ω and ρ-mesons, the Yukawa shape will be very much modified. Hence we take the $v_S^p(r_{ij})$ to be a sum of two Woods–Saxon potentials:

$$v_S^p(r) = S^p W(r) + S'^p W'(r) , \tag{2.6}$$

$$W(r) = (1 + \exp((r - R)/a))^{-1} , \tag{2.7}$$

$$W'(r) = (1 + \exp((r - R')/a'))^{-1} . \tag{2.8}$$

It is possible to obtain reasonable fits to the scattering data with $S'^p = 0$ for all p except b and bτ. The spin-orbit potential in $T = 1$ states has to have a smaller range than that of the central core to fit the scattering data. Hence we need the $W'(r)$ terms for p = b and bτ. We note that the parameterization of our interaction has similarities with that used by Hamada and Johnston [9]) and by Brussel *et al.* [10]).

The values of the parameters are determined by fitting the neutron-proton phase shifts obtained by Arndt *et al.* [11]) by energy-dependent analysis. Consideration was

given to (i) phases obtained by energy-independent analysis, (ii) a more recent analysis by Arndt [12]) of the mixing E1 in the $^3S_1$-$^3D_1$ channel, and (iii) the recent analyses of Bugg *et al.* [13]), particularly in regions where energy-dependent and independent analysis give different phases. The phase shifts up to 425 lab energy are fitted; not because we believe that a non-relativistic model is adequate at such energies, but because if one wants to correct for effects of relativistic kinematics [14]) it may be useful to start from a non-relativistic potential that indeed fits the scattering data.

There is some evidence that the NN interaction has a charge dependence. Since nuclei generally have more neutrons than protons, and neutron stars have mostly neutrons, it may be better to fit the $T = 1$ interaction to nn data. However, nn data is nonexistent, and so we fit the np data. The ^{3}He-^{3}H mass difference suggests that the nn interaction is a little more attractive than the pp [ref. [15])], and the np scattering data also suggests that the np interaction is a little more attractive than the pp interaction. From a practical point of view one does not have to compute Coulomb functions for fitting the np scattering.

In the singlet channels, the v_{14} potential takes the form (we use $v_{T,S}$ to denote potentials in states having pair isospin and spin T, S):

$$v_{T,0} = \sum_{p=c,q} (S^p_{T,0} W(r) + I^p_{T,0} T^2_\pi(r)) O^p + v_{\pi,T,0}\,; \tag{2.9}$$

whereas in triplet states:

$$v_{T,1} = \sum_{p=c,t,b,q,bb} (S^p_{T,1} W(r) + S'^p_{T,1} W'(r) + I^p_{T,1} T^2_\pi(r)) O^p + v_{\pi,T,1}\,. \tag{2.10}$$

The strenghs $S^p_{T,S}$, $S'^p_{T,S}$ and $I^p_{T,S}$ are determined from the fits, the S^p, S'^p and I^p are trivially obtained from these. The $S^p_{T,S}$ and $I^p_{T,S}$ are given in tables 1 and 2, while the complete list of parameters along with S^p and I^p is given in table 3. The I^p and S^p for p = q, qσ, qτ, q$\sigma\tau$, bb and bbτ are much smaller than those for p = c, σ, τ and $\sigma\tau$.

We compare our phase shifts with those given by the Paris potential [3]), Reid v_{12} and (Bethe Johnson) BJ-II v_{12} models. The Paris potential has a theoretically plausible two-pion-exchange contribution, which we have approximated by $v^p_1(r)O^p$. The Reid and BJ-II v_8 models have their $^1S_0$, $^3S_1$-$^3D_1$, $^1P_1$ and $^3P_2$-$^3F_2$ potentials in T, S = 1, 0; 0, 1; 0, 0 and 1, 1 states, whereas the v_{12} models have:

$$v_{1,0} = v(^1S_0) + \tfrac{1}{6}(v(^1D_2) - v(^1S_0))O^q\,, \tag{2.11}$$

TABLE 1

Potential strengths in singlet states (MeV)

p	$S^p_{1,0}$	$I^p_{1,0}$	$S^p_{0,0}$	$I^p_{0,0}$
c	2000	−6.255	8700	−13.2
q	49	0	−500	0.6

TABLE 2

Potential strengths in triplet states (MeV)

p	$S^p_{0,1}$	$S'^p_{0,1}$	$I^p_{0,1}$	$S^p_{1,1}$	$S'^p_{1,1}$	$I^p_{1,1}$
c	2400	0	−6.8009	2145	0	−4.32
t	0	0	0.75	0	0	−0.18
b	80	0	0	0	−2200	0
q	380	0	0	−20	0	0
bb	−230	0	−0.2	147.5	0	0

TABLE 3

Parameters of the v_{14} two-nucleon interaction model

p	I^p	S^p	S'^p
c	−5.7030	2575.3	0
σ	0.7628	−366.56	0
τ	0.8992	−466.56	0
$\sigma\tau$	−0.2790	402.81	0
t	0.0525	0	0
$t\tau$	−0.2325	0	0
b	0	20	−1650
$b\tau$	0	−20	−550
q	0.0375	37.938	0
$q\sigma$	−0.0375	42.063	0
$q\tau$	−0.0375	−40.688	0
$q\sigma\tau$	0.0375	−59.313	0
bb	−0.05	53.125	0
$bb\tau$	0.05	94.375	0

$c = 2\ \mathrm{fm}^{-2}$, $R = 0.5$ fm, $a = 0.2$ fm, $R' = 0.36$ fm, $a' = 0.17$ fm.

$$v_{0,1} = v(^3S_1 - {}^3D_1) + \tfrac{1}{6}(v(^1D_2) - v(^1S_0))(O^q + 2O^b)\,, \tag{2.12}$$

$$v_{0,0} = v(^1P_1)\,, \tag{2.13}$$

$$v_{1,1} = v(^3P_2 - {}^3F_2)\,. \tag{2.14}$$

The v_8 models fit the $^1S_0$, $^3S_1$-$^3D_1$, $^1P_1$ and $^3P_2$-$^3F_2$ phases; the v_{12} models fit these, the $^1D_2$, and give a reasonable value for the weighted average of ^3D phases:

$$\delta_{av}(^3D) = \tfrac{1}{15}[3\delta(^3D_1) + 5\delta(^3D_2) + 7\delta(^3D_3)]\,. \tag{2.15}$$

The operator $(O^q + 2O^b)$ in eq. (2.12) gives a zero when operating on $^3S_1$ and $^3D_1$ states, and thus the $^3S_1$-$^3D_1$ interaction is unaffected by the added term.

Figs. 1–3 show the potentials in T, S channels and compare it with the Reid v_{12} in a couple of cases. Figs. 4-19 show the AHR [Arndt *et al.* [11])] energy-dependent np

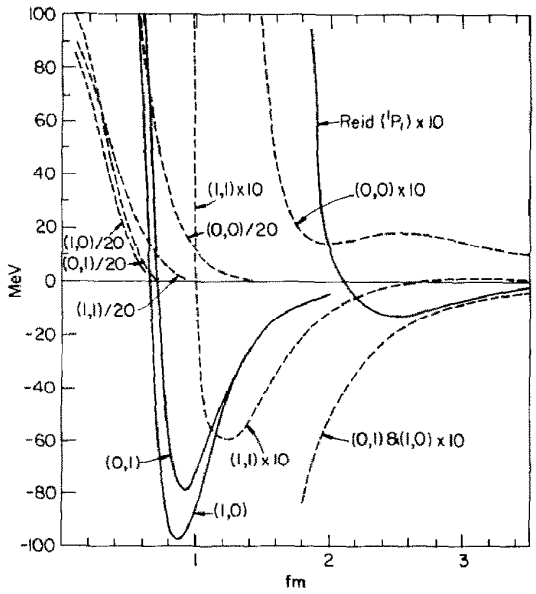

Fig. 1. The $v^{c}_{T,S}$ of the v_{14} interaction model, and the Reid $v(^1P_1)$.

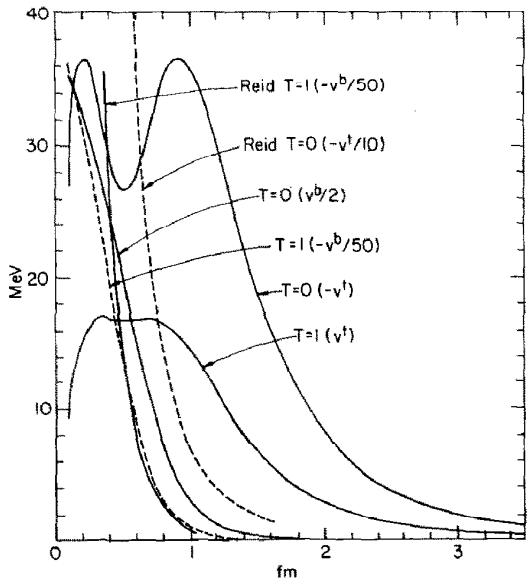

Fig. 2. The $v^{t}_{T,S}$, $v^{b}_{T,S}$, and the Reid $v^{t}(^3S_1\text{-}^3D_1)$ and $v^{b}(^3P_2\text{-}^3F_2)$.

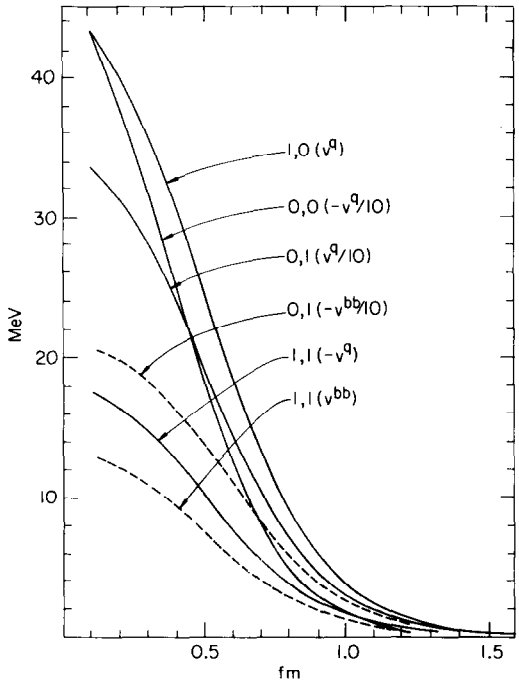

Fig. 3. The $v^q_{T,S}$ and $v^{bb}_{T,S}$.

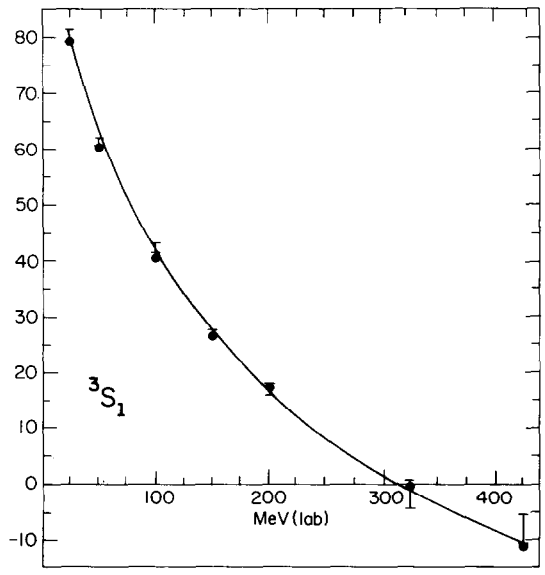

Fig. 4. The $^3S_1$ phase shifts. The full curve gives results of the energy-dependent analysis of ref. [11]), the I and ↕ give results of energy-independent anaysis of refs. [11,13]), respectively, and the points give v_{14} results.

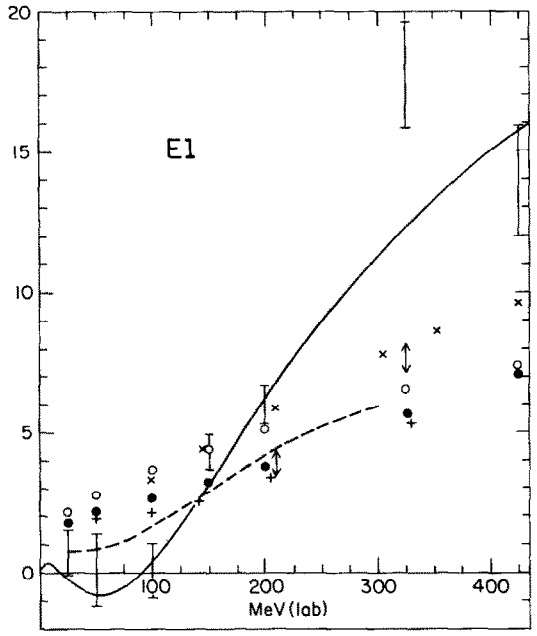

Fig. 5. The E_1 in $^3S_1$-$^3D_1$ channel. The full and broken curves give results of energy-independent analysis of refs. [11,12]), respectively; the I and ↕ of energy-independent analysis of refs. [11,13]) respectively; and the ·, +, × and ○ give v_{14}, Paris, Reid and BJ-II v_{12} phases.

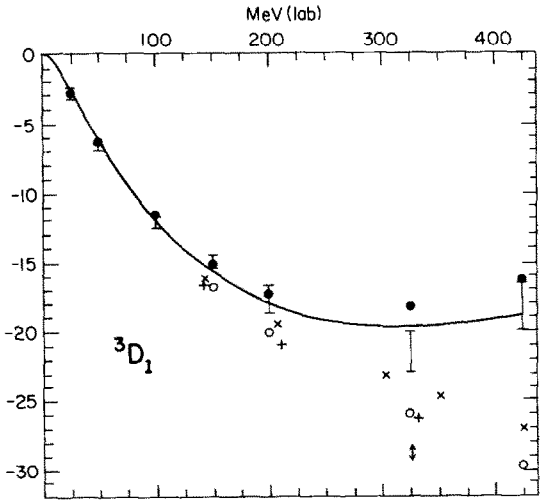

Fig. 6. The $^3D_1$ phase shifts. See fig. 5 for notation.

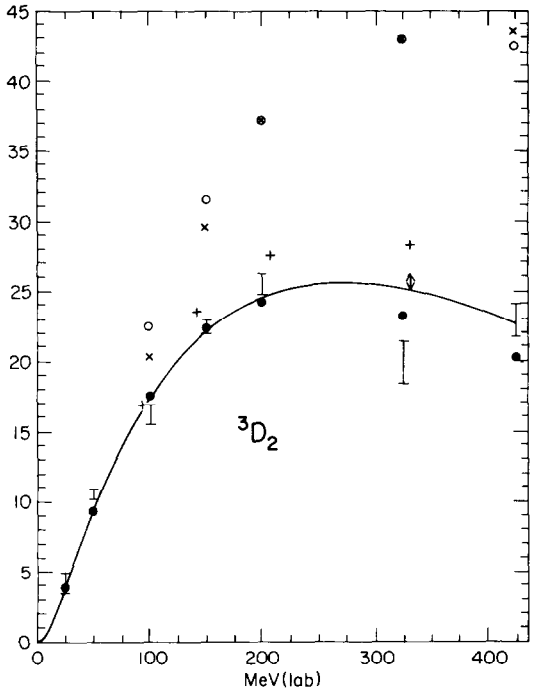

Fig. 7. The $^3D_2$ phase shifts. See fig. 5 for notation.

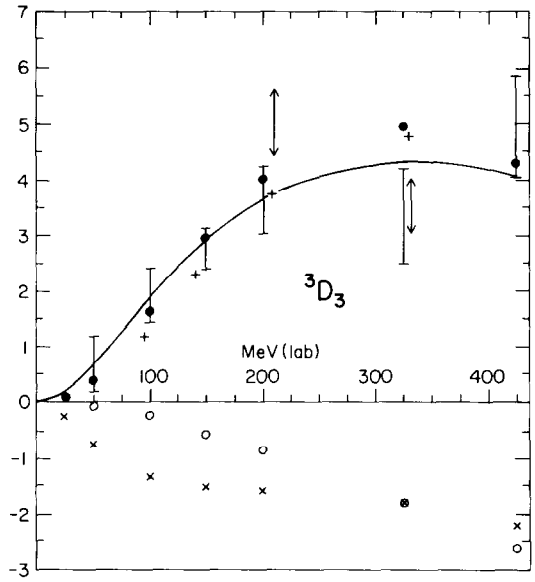

Fig. 8. The $^3D_3$ phase shifts. See fig. 5 for notation.

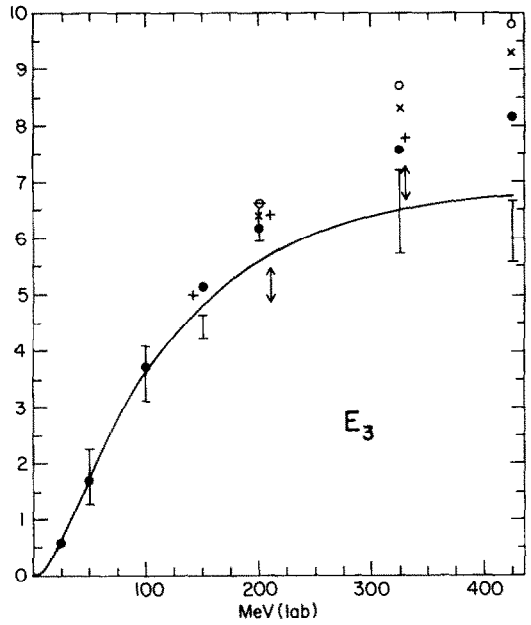

Fig. 9. The E_3 in $^3D_3$-$^3G_3$ channel. See fig. 5 for notation.

phase shifts by solid lines and energy-dependent pp phase shifts by dashed lines. The Arndt [12]) energy-dependent E1 is shown in fig. 5 by a broken line. The phases obtained by energy-independent analysis by AHR and by Bugg *et al.* [13]) are respectively shown by I, and ↕. In $T=0$ channels these are np phases, while in $T=1$ channels they are pp. The phases calculated with the present, Paris, Reid v_{12} and BJ-II v_{12} potentials are shown by ·, +, × and ○ respectively. Note that the Paris, Reid and BJ potentials are fitted to the pp phase shifts in $T=1$ states, while ours are fitted

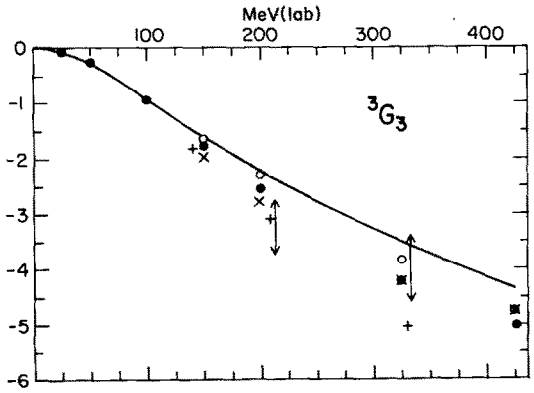

Fig. 10. The $^3G_3$ phase shifts. See fig. 5 for notation.

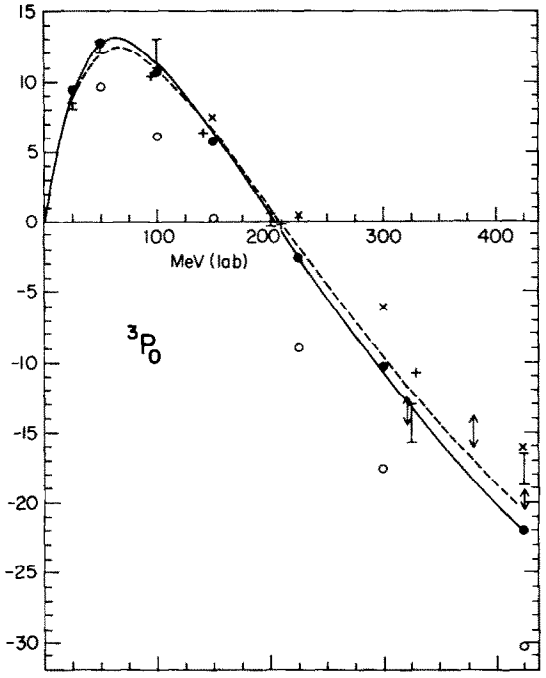

Fig. 11. The $^3P_0$ phase shifts. The full and dashed lines give the results of energy-dependent np and pp analysis of ref. [11]), respectively; the I and ↕ give results of energy-independent pp analysis of refs. [11,13]), respectively; the ·, × and ○ give np results with the v_{14}, Reid and BJ-II v_{12} models, and the + give pp Paris results.

to the np data. There is a very sizable difference between the np and pp $^1S_0$ phases at high energy.

The central potentials in the T, S channeels (fig. 1) have the familiar shape. The v^c in 0, 0 states does not become negative like Reid's (fig. 1). The Reid ($^1P_1$) potential gives very bad phase shifts in the $^1F_3$ state (fig. 19) and thus is not a proper representation of the $T, S = 0, 0$ interaction. Also note from fig. 1 that the v^c in 0, 1 states is almost but not quite as attractive as that in 1, 0 states.

The tensor potentials are much weaker than Reid's particularly at $r \leqslant 1$ fm. They are given by a sum of two terms:

$$v^t_{T,1} = I^t_{T,1} T^2_\pi(r) + 3.488(4T-3) T_\pi(r)\,, \tag{2.16}$$

and $T_\pi(r)$ is linear in r at small r. The two terms of $v^t_{T,1}$ have opposite signs, and so the $v^t_{T,1}$ have an unreasonable peak at ~0.2 fm. This peak is purely due to our choice of cut-off and should not have any physical significance; neither does it have any effect on the two-nucleon interaction. The Reid v_{12} potential has a very strong tensor force as can be seen from the $^3D_1$, $^3D_2$ and $^3D_3$ phase shifts shown in figs. 6–8. The tensor force is attractive in $^3D_2$, while repulsive in $^3D_1$ and $^3D_3$ states.

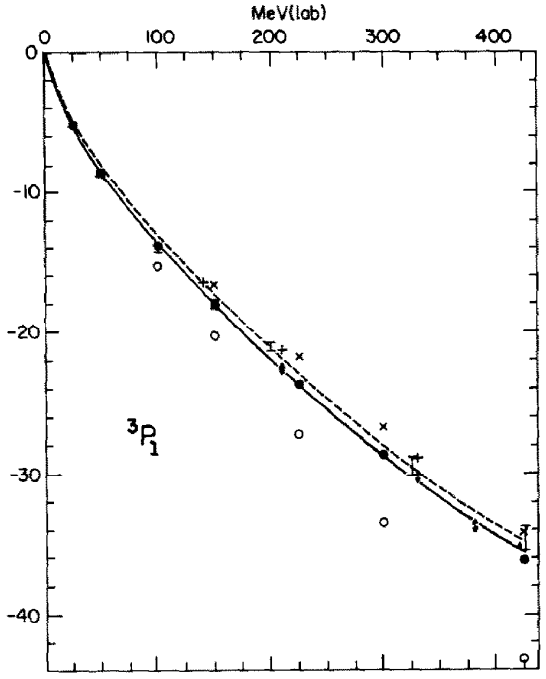

Fig. 12. The $^3P_1$ phase shifts. See fig. 11 for notation.

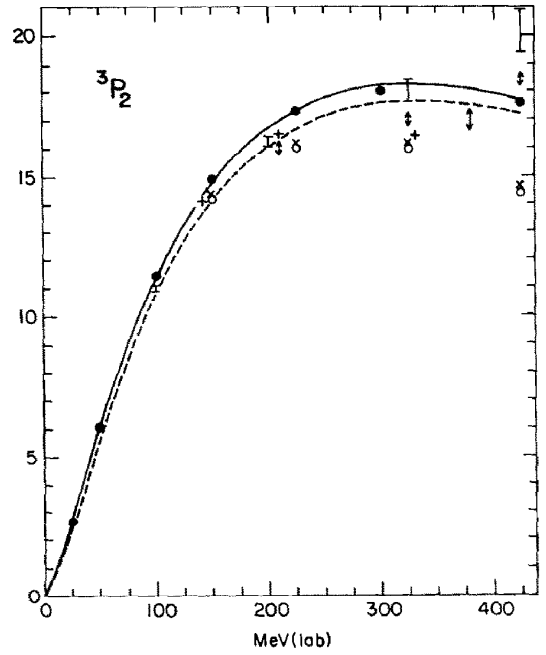

Fig. 13. The $^3P_2$ phase shifts. See fig. 11 for notation.

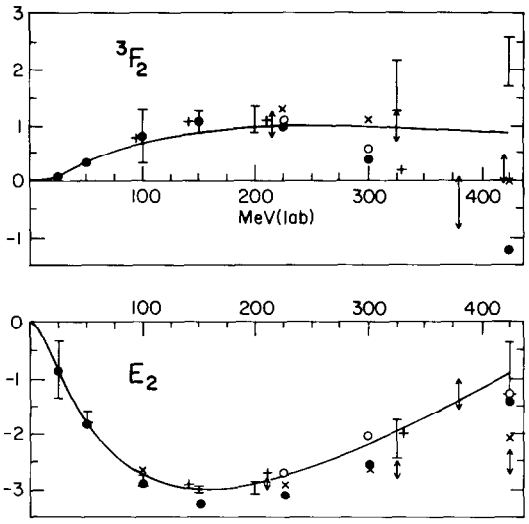

Fig. 14. The $^3F_2$ phase shifts and E_2 in $^3P_2$-$^3F_2$ channel. See fig. 11 for notation.

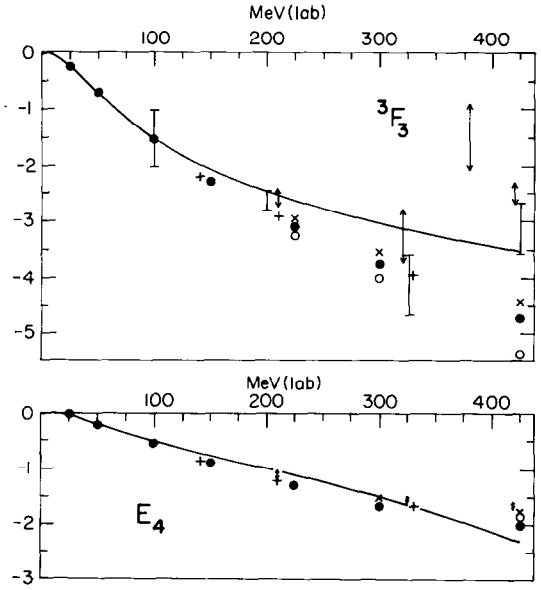

Fig. 15. The $^3F_3$ phase shifts and E_4 in $^3F_4$-$^3H_4$ channel. See fig. 11 for notation.

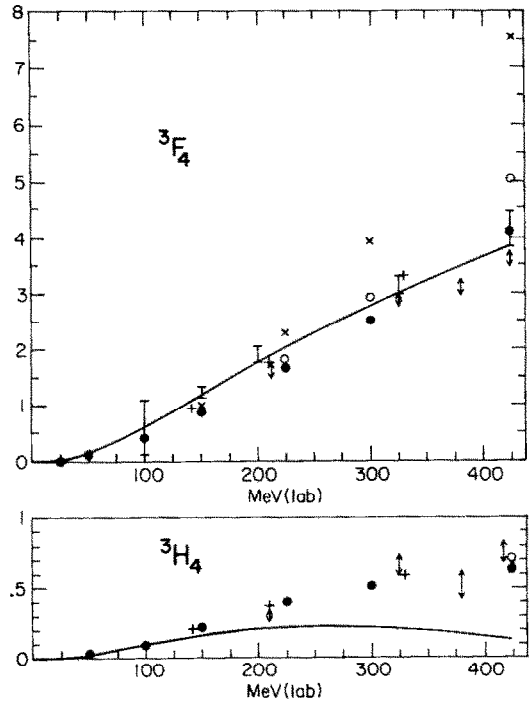

Fig. 16. The $^3F_4$ and $^3H_4$ phase shifts. See fig. 11 for notation.

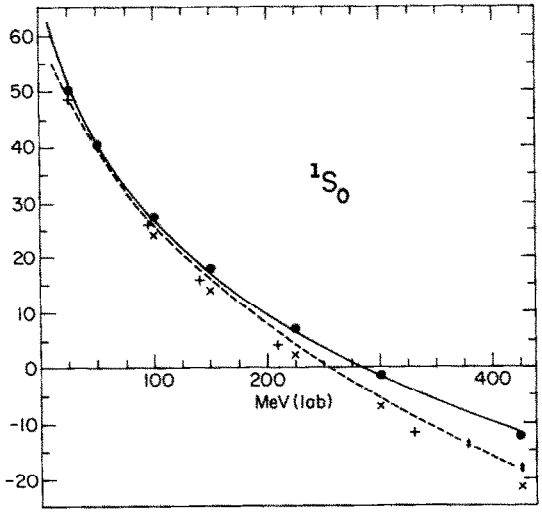

Fig. 17. The $^1S_0$ phase shifts. See fig. 11 for notation.

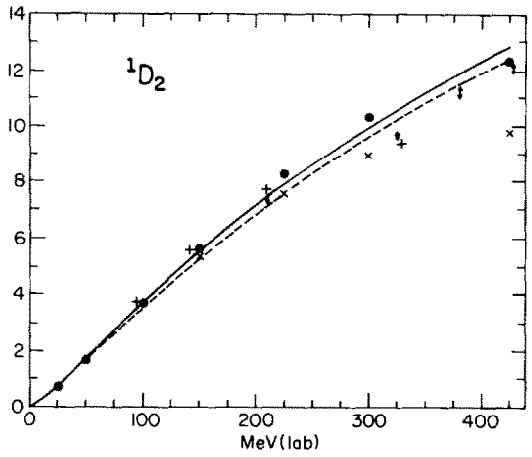

Fig. 18. The $^1D_2$ phase shifts. See fig. 11 for notation.

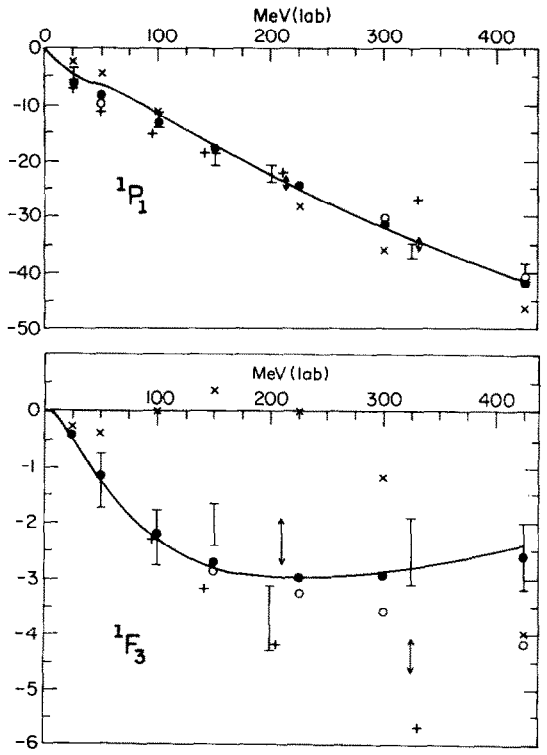

Fig. 19. The $^1P_1$ and $^1F_3$ phase shifts. See fig. 5 for notation.

The $\boldsymbol{L}\cdot\boldsymbol{S}$ interaction (fig. 2) in $T=0$ states is weak, while that in $T=1$ states is comparable with Reid's. The BJ-II v_{12} potential has a very strong $\boldsymbol{L}\cdot\boldsymbol{S}$ interaction in $T=1$ states, and it fails to explain the scattering data in $^3P_0$ and $^3P_1$ states (figs. 11, 12). The Reid v_8, v_{12} models also do not explain $^3P_0$ and $^3P_1$ phases very satisfactorily. The range of the $\boldsymbol{L}\cdot\boldsymbol{S}$ potential in $T=1$ states has to be shorter than the range of the repulsive core in $T, S=1, 1$ states to (i) reproduce the $^3P_2$ phase shift (fig. 13) at higher energies, and (ii) to prevent the $^3F_4$ phase (fig. 16) from becoming too attractive at $E\sim 400$ MeV.

The L^2 and $(\boldsymbol{L}\cdot\boldsymbol{S})^2$ potentials are shown in fig. 3. In triplet states the $v^{q}_{T,S}$ and $v^{bb}_{T,S}$ have opposite signs, and they cancel substantially in the $J=l+1$ channels. The $v^{q}_{0,1}$ and $v^{bb}_{0,1}$ are needed primarily to reduce the large attractive phase shifts in $^3D_2$ without making the $^3D_1$ and $^3D_3$ phases very repulsive. The $v^{q}_{1,0}$ is well determined by the $^1D_2$ phase (fig. 18), and it is quite small. In principle the ^3F phases could determine the $v^{q}_{1,1}$ and $v^{bb}_{1,1}$, but the data on $^3F_2$ and $^3F_3$ phases is rather poor. Fortunately the $v^{q}_{1,1}$ and $v^{bb}_{1,1}$ appear to be very weak. A relatively substantial $v^{q}_{0,0}$ is needed to fit the $^1F_3$ phase (fig. 19), however the data here is not too good.

The data on E1 (fig. 5) is also poor. If we had chosen an even weaker tensor force in $T=0$ states, the E1 would have become smaller, and the ^3D phases could be fit with weaker $v^{q}_{0,1}$ and $v^{bb}_{0,1}$. Thus E1 plays an important role in deducing the interaction operator from the scattering data, and a better measurement of it will be most welcome.

In general our phases are not too different from those given by the Paris potential. We seem to do a little better on the spin singlet states and the ^3P states, while the data on ^3D and ^3F states is not accurate enough to choose among the two models. However, it must be noted that the Paris potential is fitted to the scattering data itself whereas ours is fitted to phase shifts.

The contribution of Δ (33-resonances) to I^c can be estimated in the closure approximation [7]). It comes out to ~ -2, whereas the I^c in our model is -5.7 (table 3). Hence it is suggested that the Δ's provide only a third or so of the intermediate range attraction. The rest of it must be from other resonances, and the $\pi\pi$ interactions. However it should be pointed out that I^c is not uniquely determined by the data. It is possible to make substantial correlated changes in the parameters I^c, c, R and S^c which leave the phases relatively unaffected. The values of $I^{p\neq c}$ are much smaller than I^c in accord with the isobar model.

3. The deuteron properties

The calculated deuteron energy, quadrupole moment, D-state probability, and the asymptotic D- to S-state ratio [21]) are given in table 4, along with their experimental values, and those obtained with the Paris and Reid models. Thanks to the weaker tensor force the D-state percentage is small, but not quite as small as suggested by the

TABLE 4

Deuteron properties

	Present	Paris	Reid	Exp
E (MeV)	−2.225	−2.225	−2.225	−2.224
Q (fm^2)	0.273	0.279	0.280	0.278 ± 0.008
D-state (%)	5.2	5.8	6.5	<5?
A_D/A_S	0.025	0.026	0.026	0.263 ± 0.0013

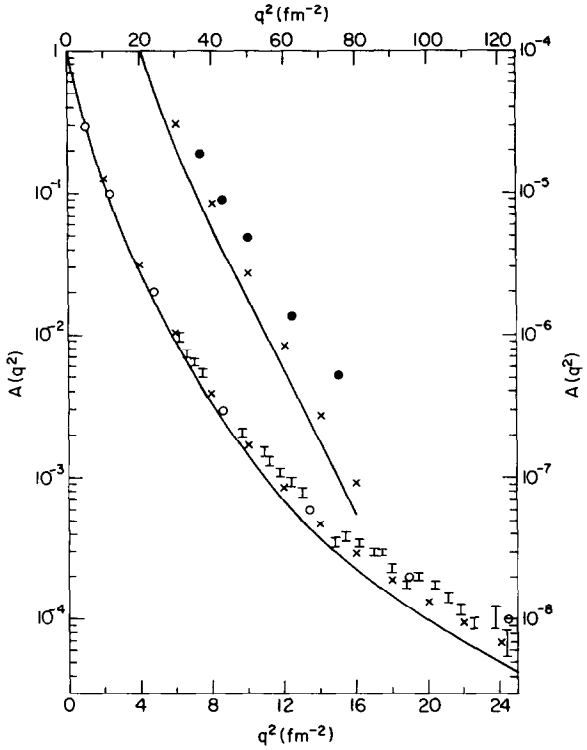

Fig. 20. The deuteron $A(q^2)$. The full curve, × and ○'s give results obtained with the v_{14}, Reid v_{12} and Paris potentials respectively; the I's are experimental results from ref. [16]) and literature cited therein, while the · are from ref. [17]). The top and right side scale is for the top curve, and the bottom and left side scale is for the bottom curve.

photodisintegration data [20]). The quadrupole moment and the A_D/A_S are both on the lower side, but within experimental limits.

In fig. 20 we compare the calculated deuteron structure function $A(q^2)$ with the experiment [16,17]), and predictions of Paris and Reid models. The $A^2(q)$ is underestimated by ~10% at $q^2 = 6$ fm^{-2}, and by ~33% at $q^2 \sim 20$. Of course there is no reason to believe our non-relativistic calculation at $q^2 \gtrsim 10$.

The "dipole" approximation

$$F_0(q) = 1/(1+aq^2)^2\,, \qquad a = 0.055\ \mathrm{fm}^{-2}\,, \tag{3.1}$$

is used for the proton form factor in the calculation of $A(q^2)$. Using the more realistic $F_0(q)$ of Blatnik and Zovko [18]) will increase our $A^2(q)$ in the $q^2 = 20\ \mathrm{fm}^{-2}$ region by a few percent.

Instead of taking into account the nucleon isobar degrees of freedom by an effective intermediate range attraction $v_I^p(r_{ij})O_{ij}^p$, if they are explicitly included in the deuteron wave function, the $A(q^2)$ will probably be a few percent larger in the $q^2 \sim 10\ \mathrm{fm}^{-2}$ region [19]) It is also likely that the meson-exchange-current (MEC) contributions will increase $A(q^2)$ somewhat.

Both Paris and Reid potentials do better on the $A(q^2 \lesssim 20\ \mathrm{fm}^{-2})$, probably because they have somewhat stronger tensor force than ours. However, the deuteron photodisintegration data [20,21]) supports a tensor force that is even weaker than ours ($P_D < 5\%$). It appears to be rather difficult to simultaneously obtain (i) the correct ^3D_J phases with weak $v_{0,1}^q$ and $v_{0,1}^{bb}$, (ii) the correct $A(q^2 \lesssim 10\ \mathrm{fm}^{-2})$ and (iii) a $P_D \lesssim 5\%$. In our model we have compromised a little on both P_D and $A(q^2)$ hoping that isobar and meson-exchange-current corrections will have some effect on the interpretation of the electron scattering and photodisintegration data.

References

1) R.V. Reid, Ann. of Phys. **50** (1968) 411
2) H.A. Bethe and M.B. Johnson, Nucl. Phys. **A230** (1974) 1
3) M. Lacombe, B. Loiseau, J.M. Richard, R. Vinhmau, J. Côté, P. Pirés and R. de Tourreil, preprint (1979)
4) O.V. Maxwell and R.A. Smith, Nucl. Phys. **A338** (1980) 105
5) I.E. Lagaris and V.R. Pandharipande, Nucl. Phys. **A359** (1981) 349
6) A.M. Green, Rep. Prog. Phys. **39** (1976) 1109
7) R.A. Smith and V.R. Pandharipande, Nucl. Phys. **A256** (1976) 327
8) A.M. Green and P. Haapakoski, Nucl. Phys. **A221** (1974) 429
9) T. Hamada and I.D. Johnston, Nucl. Phys. **34** (1962) 382
10) C.N. Brussel, A.K. Kerman and B. Rouben, Nucl. Phys. **A124** (1969) 624
11) R.A. Arndt, R.H. Hackman and L.D. Roper, Phys. Rev. **C15** (1977) 1002
12) R.A. Arndt, Private communication (1978) (quoted in ref. [3])
13) D.V. Bugg, J.A. Edgington, C. Amster, R.C. Brown, C.J. Oram and K. Shakarchi, J. of Phys. **G4** (1978) 1025
    D.V. Bugg, J.A. Edgington, W.R. Gibson, N. Wright, N.M. Stewart, A.S. Clough, D. Axen, G.A. Ludgate, C.J. Oram, L.P. Robertson, J.R. Richardson and C. Amsler, preprint (1979)
14) G.E. Brown, A.D. Jackson and T.T.S. Kuo, Nucl. Phys. **A133** (1969) 481
15) A.C. Phillips, Rep. Prog. Phys. **40** (1977) 905
16) S. Galster, H. Klein, J. Moritz, K.H. Schmidt, D. Wegener and J. Bleckwenn, DESY report 71/7 (1971)
17) R.G. Arnold, B.T. Chertok, E.B. Dally, A. Grigorian, C.L. Jordan, W.P. Schütz, R. Zdarko, F. Martin and B.A. Mecking, Phys. Rev. Lett. **35** (1975) 776
18) S. Blatnik and N. Zovko, Acta Phys. Austriaca **39** (1974) 62
19) H.J. Weber and H. Arenhövel, Phys. Reports **36C** (1978) 277
20) H. Arenhövel and W. Fabian, Nucl. Phys. **A282** (1977) 397
21) H.E. Conzett, F. Hinterberger, P. von Rossen, F. Seiter and E.J. Stephenson, Phys. Rev. Lett. **43** (1979) 572